表2 凍結卵子由来児の予後

	緩速凍結法	ガラス化法
報告数	23	9
融解卵子	11,890	5435
生存	8056 (68%, 22~90)	4392 (81%, 69~91)
受精(2PN)	(73%, 50~86)	(79%, 59~93)
胚移植	1974	834
出生児	282	295
児獲得率(%)	2.3%	5.2%
男女比	1.070	1.119
先天異常	VSD, choanal atresia, Rubinstein-Taibi 症候群	VSD(2), 結腸管閉鎖, clubfoot, 海綿状血管腫

(Noyes N, et al : Reprod Biomed Online, 2009[10]より改変)

フリーザーが不要で，凍結にかかる時間も短くて簡便なガラス化法が，今後さらに普及することは明らかであろう．

3．卵胞期や黄体期であっても卵子凍結は不可能ではない

悪性腫瘍治療の場合，治療をすぐに始めなければならない場合が多く，たとえ自然周期でも排卵期を待っていることができないことがある．このような場合，卵胞期や黄体期に採取した未成熟卵を体外成熟させて凍結保存する方法が考えられている．

卵胞期に採取した未成熟卵については，PCO患者で採取卵子を体外成熟・凍結融解後にICSIして妊娠した例がすでに報告されている[11]．この症例は悪性腫瘍患者ではないが，原病による影響を受けていない症例で，かつある程度の卵胞成熟が認められる時期であれば，場合によっては試みてよい方法であると考えられる．

また，黄体期に採取した卵子についても，最近の報告で3例の悪性腫瘍治療前の患者から採取した黄体期GV期卵子を体外成熟させて得られたMII期卵子を凍結しているものがある[12]．この報告では，3例からそれぞれ7，5，7個の卵子がhCG注射後36時間で採取され，それぞれ5，3，5個の体外成熟MII卵子が凍結されている．黄体期に採取された卵子の妊孕性がどの程度あるかは不明であるが，黄体期に採取した卵子を体外成熟させた初期のChaらの報告[13]や，黄体期の延長である帝王切開時に採取された卵子を提供卵子とした妊娠例の報告[14]があることから，確率はともかく可能性としてはあると考えられる．

4．卵巣凍結保存は悪性細胞再移植の危険性が問題である

卵巣凍結による妊孕性保存の長所は，第一に多数の卵子を保存できる可能性があること，第二に性周期や自然妊娠を含めて卵巣機能そのものを保存することができることである．ヒト卵巣凍結では，凍結保存した卵巣組織を融解後自家正所移植，つまり患者の卵巣が元あった部位(後腹膜，あるいは残存卵巣上)に移植する方法で，これまで文献上，世界で数例の妊娠・出産例の報告がなされており，現在までに報告されている妊娠例はすべて緩慢凍結法によっている[15]．緩慢凍結法では，卵巣皮質を2mm角，あるいは10×5×2mm程度の短冊状に切り出して，1.5M DMSOを凍結保護剤としてプログラムフリーザーで緩慢凍結する．一方，最近わが国の香川・桑山らによって開発されたガラス化法は，10mm×10mm×1mmの卵巣切片を作成し，特殊な容器を用いて液体窒素に直接投入して凍結するもので，緩慢法に

比して卵胞への凍結障害に加えて卵胞への形態学的な障害が少ないと報告されている[16]．この方法では，間質の障害も少ないと報告されていることから，後述する機能期間の延長にも今後期待が持たれる[17]．

卵巣凍結の問題点として，第一に現在の技術では有効に保存できる卵胞数が少ないこと，第二に融解後移植する卵巣に悪性細胞が含まれる危険性があることがあげられる．

第一の問題点については，融解後に卵巣組織片が機能する期間が短いという事実によって推測される．この主たる原因は，融解後，自家移植する卵巣片が生着するまで血流が途絶していることによると言われており，この阻血期間(低酸素状態となる)に多くの卵胞が死滅するとされている．解決法として，現在は移植の1～2週間前に移植部(後腹膜など)に手術操作を行ってあらかじめ血管新生を促しておき，移植後の阻血時間を短くしようという試みがなされているが，画期的な方法とはなっていない．別の方法として，血管をつけたままで卵巣を(皮質片とせず)そのまま凍結する方法が考えられているが，この方法の問題点はもし血管が血栓などで閉塞しまうと全卵巣機能が失われることにあり，動物実験でどの程度の割合で生着するかが明らかにならないと臨床応用は困難と考えられる．結局，現時点では皮質片の移植後の卵胞生存率を高めるのが現実的と考えられる．

第二の問題点である悪性細胞再移植については，すでに1996年にlymphomaを発症させた雌の卵巣を別のrecipient雌に移植したところ，recipient雌はlymphomaを発症，9～43日後に死亡したという報告がある[18]．ヒトでは，これまでのところ悪性細胞再移植の実例は確認されていないが，考慮しなければならない危険であり，緩速法であってもガラス化法であっても自家移植をする限り，その危険性は決して0にはならない．

悪性細胞再移植の危険性を解決するには，自家移植による卵胞発育を避けるため，異種移植，あるいは卵巣組織や単離した未熟卵胞の体外培養系の確立が必要である．しかし，異種移植は，ヒト卵巣を移植した動物からの母胎・あるいは胎児への病原菌感染の危険性があり，一方卵巣組織・未熟卵胞の体外培養はマウスなどの齧歯類で少数の成功例が報告されているものの，その発育率がきわめて低いことから，臨床応用されるにはかなり長い期間が必要と考えられる．そこで，現在卵巣凍結時に同時に卵子を凍結保存する方法が考えられている(次項)．

5．卵巣組織凍結時の非刺激GV期卵子の利用

卵巣組織凍結の最大の問題点は悪性細胞再移植の危険性であり，もし凍結卵巣組織に悪性細胞を認めれば，凍結した卵巣組織の自家移植は不可能となる．しかし，卵巣凍結時に一定数の卵子を凍結することができれば，このような卵巣凍結の弱点をカバーできる．

一方，成熟卵子凍結に必要な卵巣刺激や，hCG投与による卵巣過剰刺激症候群は，悪性腫瘍の治療開始を遅らせてしまう．また，乳癌などのホルモン感受性腫瘍では刺激自体が原病を増悪させる可能性がある．しかし，非刺激GV期卵を妊孕性温存治療に利用できるとすれば，体内のホルモン状態を変化させず，また原病治療開始までの時間を延長させず，さらに妊孕性保存を行わなければならない場合でも月経周期に関係なく卵子を得ることができる．

GV期卵子を妊孕性保存に利用する際の安全性に関しては，主にPCO症例に対してhCG刺激を行って得たGV期卵子由来の子どもについてはすでに多数出産例があり，異常は増加しないと報告されている[19]．また，ウシ・ブタなどの畜産動物では，産仔作出のための卵子は屠場由来の非刺激卵巣から採取したGV期卵子が一般的に用いられ，これによって産仔の異常が増加するという報告はないことからも，実験的技術ではあるが許容できる範囲であると考えられる．そこで，卵巣凍結時に摘出卵巣からGV期卵子を採取し，これを妊孕性保存に利用する試みが行われている．

得られたGV期卵子は，通常体外成熟させ，MII期になったものを凍結する．ただ，体外成熟

の成功率や得られた卵子の妊孕性は，成熟卵子と比べるとまだ満足すべき率ではない．この低い発生率の一因は，GV期卵子の体外培養法が現在開発途上であり，市販の培養液の体外成熟率が低いことにあると考えられる．そこで，わが国でもっとも多数の卵巣凍結症例をもつ施設の一つである加藤レディースクリニックの香川らは，将来GV期卵の体外成熟技術が改善されることを期待して，GV期卵をそのままガラス化法にて凍結するという新しい方法を臨床に用いている(personal communication)．マウスでは，凍結保存GV期卵から体外培養・体外受精を行って産仔を得たという報告があり，さらにガラス化法によって融解後の発生率は高くなると報告されていることから[20]，一つの有望な方法と考えられる．

いずれにしても，卵巣凍結時のGV期卵子の利用は，とくに卵巣に高率に転移する乳癌患者などを中心に，有望な妊孕性保存法となると考えられる．

文　献

1) Chung K, Irani J, Knee G, et al : Sperm cryopreservation for male patients with cancer : an epidemiological analysis at the University of Pennsylvania. Eur J Obstet Gynecol Reprod Biol 113 (Suppl 1) : S7−11, 2004.
2) Schrader M, Müller M, Sofikitis N, et al : "Oncotese" : testicular sperm extraction in azoospermic cancer patients before chemotherapy-new guidelines ? Urology 61(2) : 421−425, 2003.
3) Brinster RL, Avarbock MR : Germline transmission of donor haplotype following spermatogonial transplantation. Proc Natl Acad Sci USA 91 (24) : 11303−11307, 1994.
4) Keros V, Hultenby K, Borgström B, et al : Methods of cryopreservation of testicular tissue with viable spermatogonia in pre-pubertal boys undergoing gonadotoxic cancer treatment. Hum Reprod 22(5) : 1384−1395, 2007.
5) Ginsberg JP, Carlson CA, Lin K, et al : An experimental protocol for fertility preservation in prepubertal boys recently diagnosed with cancer : a report of acceptability and safety. Hum Reprod 25(1) : 37−41, 2010.
6) Kavoussi SK, Fisseha S, Smith YR, et al : Oocyte cryopreservation in a woman with mosaic Turner syndrome : a case report. J Reprod Med 53 : 223−226, 2008.
7) Huang J, Tulandi T, Holzer H, et al : Cryopreservation of ovarian tissue and in vitro matured oocytes in a female with mosaic Turner syndrome ; case report. Hum Reprod 23 : 336−339, 2008.
8) Porcu E, Fabbri R, Damiano G, et al : Clinical experience and applications of oocyte cryopreservation. Mol Cell Endocrinol 169(1 - 2) : 33−37, 2000.
9) Kuwayama M, Vajta G, Kato O, et al : Highly efficient vitrification method for cryopreser-vation of human oocytes. Reprod Biomed Online 11(3) : 300−308, 2005.
10) Noyes N, Porcu E, Borini A : Over 900 oocyte cryopreservation babies born with no apparent increase in congenital anomalies. Reprod Biomed Online 18(6) : 769−776, 2009.
11) Chian RC, Gilbert L, Huang JY, et al : Live birth after vitrification of in vitro matured human oocytes. Fertil Steril 91(2) : 372−376, 2009.
12) Demirtas E, Elizur S, Holzer H, et al : Case report : immature oocyte retrieval in the luteal phase to preserve fertility in cancer patients. Reprod Biomed Online 17 : 520−523, 2008.
13) Cha KY, Do BR, Chi HJ, et al : Viability of human follicular oocytes collected from unstimulated ovaries and matured and fertilized in vitro. Reproduction, Fertility and Development 4 : 695−701, 1992.
14) Hwang JL, Lin YH, Tsai YL : Pregnancy after immature oocyte donation and intracytoplasmic sperm injection. Fertil Steril 68(6) : 1139−1140, 1997.
15) Donnez J, Dolmans MM, Demylle D, et al : Live-birth after orthotopic transplantation of cryopreserved ovarian tissue. Lancet 364(9443) : 1405−1410, 2004.
16) Kagawa N, Silber S, Kuwayama M : Successful vitrification of bovine and human ovarian tissue. Reprod Biomed Online 18(4) : 568−577, 2009.
17) Silber S, Kagawa N, Kuwayama M, et al : Duration of fertility after fresh and frozen ovary transplantation. Fertil Steril 2010[Epub ahead of print]
18) Shaw JM, Bowles J, Koopman P, et al : Fresh and cryopreserved ovarian tissue samples from donors with lymphoma transmit the cancer to graft recipients. Hum Reprod 11(8) : 1668−1673, 1996.
19) Chian RC, Buckett WM, Tan SL : In-vitro maturation of human oocytes. Reprod Biomed Online 8 : 148−166, 2004.
20) Aono N, Abe Y, Hara K, et al : Production of live offspring from mouse germinal vesicle-stage oocytes vitrified by a modified stepwise method, SWEID. Fertil Steril 84(Suppl 2) : 1078−1082, 2005. ?

Animal Science Journal
Animal Science Journal (2012) **83**, 260–262 doi: 10.1111/j.1740-0929.2011.01000.x

RAPID COMMUNICATION

Common nucleotide sequence of structural gene encoding fibroblast growth factor 4 in eight cattle derived from three breeds

Sho SATO,[1] Toshikiyo TAKAHASHI,[2] Hiroshi NISHINOMIYA,[2] Makiko KATOH,[2] Ryu ITOH,[2] Masaki YOKOO,[1] Mari YOKOO,[1] Momoe IHA,[1] Yuki MORI,[1] Kano KASUGA,[1] Ikuo KOJIMA[1] and Masayuki KOBAYASHI[1]

[1]*Graduate School of Bioresource Sciences, Akita Prefectural University, Akita, and* [2]*Livestock Experiment Station, Akita Prefectural Agriculture, Forestry and Fisheries Research Center, Daisen, Japan*

ABSTRACT

Fibroblast growth factor 4 (*FGF4*) is considered as a crucial gene for the proper development of bovine embryos. However, the complete nucleotide sequences of the structural genes encoding *FGF4* in identified breeds are still unknown. In the present study, direct sequencing of PCR products derived from genomic DNA samples obtained from three Japanese Black, two Japanese Shorthorn and three Holstein cattle, revealed that the nucleotide sequences of the structural gene encoding *FGF4* matched completely among these eight cattle. On the other hand, differences in the nucleotide sequences, leading to substitutions, insertions or deletions of amino acid residues were detected when compared with the already reported sequence from unidentified breeds. We cannot rule out a possibility that the structural gene elucidated in the present study is widely distributed in cattle. To the best of our knowledge, this is the first determination of the complete nucleotide sequence of the structural gene encoding bovine *FGF4* in identified breeds.

Key words: *amino acid sequence, cattle, FGF4, fibroblast growth factor 4, structural gene.*

INTRODUCTION

In mice, fibroblast growth factor 4 (FGF4) secreted from the inner cell mass, founder cells for the epiblast, of blastocysts maintains the polar trophectoderm in a proliferative state (Tanaka *et al.* 1998). Immediately after implantation, FGF4 secreted from the epiblast stimulates the proliferation of extraembryonic ectoderm derived from the polar trophectoderm (Niswander & Martin 1992; Feldman *et al.* 1995; Tanaka *et al.* 1998). With the progression of embryogenesis, the epiblast and extraembryonic ectoderm give rise to the fetus and the placenta, respectively. Therefore, FGF4 is a crucial growth factor especially for the development of the placenta in a mouse embryo, and *Fgf4* null mice show a peri-implantation lethal phenotype (Feldman *et al.* 1995).

High rates of early embryonic, neonatal or postnatal abnormalities have consistently been observed in bovine cloning (Cibelli *et al.* 1998; Kato *et al.* 1998). Recently, aberrant expression patterns of genes, including *FGF4*, were detected in bovine embryos derived from somatic cell nuclear transfer (Amarnath *et al.* 2007; Fujii *et al.* 2010). Accordingly, *FGF4* seemed to be a crucial gene for the proper development of not only mouse embryos but also bovine embryos. However, the complete nucleotide sequence of the structural gene encoding bovine FGF4 already reported (GenBank accession no. U15969, Yu *et al.* 1995) was derived from unidentified breeds.

In this study, we identified a common structural gene encoding *FGF4* by determining the complete nucleotide sequences in three Japanese Black (JB), two Japanese Shorthorn (JS), and three Holstein (HO) cattle.

MATERIALS AND METHODS

Preparation of genomic DNA

Blood samples collected with heparin from two JB, two JS and three HO cows, were centrifuged at 4°C (1400 × *g*, 15 min). Genomic DNA was extracted from buffy-coat cells

Correspondence: Masayuki Kobayashi, Laboratory for Advanced Animal Cell Technology, Graduate School of Bioresource Sciences, Akita Prefectural University, Akita 010-0195, Japan. (Email: makoba@akita-pu.ac.jp)
Received 24 May 2011; accepted for publication 13 October 2011.

obtained from centrifuged samples and freeze-thawed sperm cells collected from one JB bull using a NucleoSpin Tissue Kit (Macherey-Nagel, Duren, Germany) in accordance with the manufacturer's instructions. These JB, JS and HO cattle were confirmed as being unrelated within the respective breeds at least for one-, three- and two-generations, respectively.

Determination of the complete nucleotide sequences of the structural gene for bovine *FGF4*

The genomic DNA region containing the complete structural gene for bovine *FGF4* was amplified by PCR as follows. Genomic DNA samples prepared in the present study were used as templates. PCR amplifications were performed in a 20-μL reaction volume with 200 ng of template, KOD-plus DNA polymerase (Toyobo, Osaka, Japan), and a primer set (5′-CACCCACGGACGCACGGCCCGAGGGCGGGG-3′, forward primer; 5′-GGGGGTTGCTTTTGTTCTTCCA-3′, reverse primer). PCR was performed as follows: hot start 2.5 min at 98°C followed by 50 cycles of 10 s at 98°C, 30 s at 54°C and 2.5 min at 68°C, and a final extension for 5 min at 68°C. PCR products were separated by 1% low melting point agarose gel electrophoresis and purified from excised gel pieces using a NucleoSpin Extract II Kit (Macherey-Nagel) in accordance with the manufacturer's instructions. Nucleotide sequences of the purified DNA fragments were determined using a BigDye Terminator v3.1 Cycle Sequencing Kit (Applied Biosystems Japan, Tokyo, Japan) in accordance with the manufacturer's instructions.

RESULTS AND DISCUSSION

The complete nucleotide sequences of PCR products (~2.2 kb) containing the full-length structural gene for *FGF4* comprised of three coding exons were determined, in addition to two introns. The nucleotide sequences have been submitted to DDBJ/EMBL/GenBank databases under the accession numbers AB633205, AB633206 and AB633207 for HO, AB633208, AB633209 and AB633210 for JB, and AB633211 and AB633212 for JS cattle. As shown in Figure 1, the deduced primary sequences of the FGF4 protein were completely identical among the JB, JS and HO cattle examined. The nucleotide sequences of their protein coding regions also completely matched. The amino acid sequence deduced from the previously reported nucleotide sequence, U15969, contained two substitutions, A6T (from GCG to ACG) and R57G (from CGC to GGC), with the letter after the number indicating the amino acid residue for U15969, one amino acid residue insertion of a leucine residue (CTG) between positions 54 and 55 for JB, JS and HO cattle, and one deletion (GCG) A31- ('-' indicates no corresponding amino acid residue in U15969). The incomplete amino acid sequence deduced from results of whole-genome shotgun sequencing (AAFC03111659 derived from Hereford genome, Zimin *et al.* 2009) is also indicated, while there were no differences from each other. From these results, nucleotide sequences leading to a common primary sequence for FGF4 protein were elucidated in all JB, JS and HO cattle examined. To date, primers for RT-PCR analysis of bovine *FGF4* transcript have been designed (Degrelle *et al.* 2005; Amarnath *et al.* 2007; Fujii *et al.* 2010; Rodriguez-Alvarez *et al.* 2010) from that in U15969. Thus, it is noteworthy that differences in nucleotide sequences are valuable, basic scientific knowledge for such analyses. On the other hand, in introns of the *FGF4* gene, differences in nucleotide

```
                                                    ▼
JB, JS and HO      1  MAGPGAAAAALLPAVLLAVLAPWAGRGGAAAPTAPNGTLEAELERRWESLVARS-LARLP  59
U15969             1  .....T.....................-.....................L..G..  59
HE (AAFC03111659)

JB, JS and HO     60  VAAQPKEAAVQSGAGDYLLGIKRLRRLYCNVGIGFHLQVLPDGRIGGVHADTSDSLLELS 119
U15969            60  ............................................................ 119
HE (AAFC03111659)  1                                                      ......   6

JB, JS and HO    120  PVERGVVSIFGVASRFFVAMSSRGRLYGSPFFTDECRFREILLPNNYNAYECDRHPGMFI 179
U15969           120  ............................................................ 179
HE (AAFC03111659)  7  ............................................................  66

JB, JS and HO    180  ALSKNGKAKKGNRVSPTMKVTHFLPRL                                 206
U15969           180  ............................                                 206
HE (AAFC03111659)  67  ............................                                  93
```

Figure 1 Alignment of the deduced primary sequences of bovine FGF4 proteins. FGF4 genes used in this alignment are from three Japanese Black (JB), two Japanese Shorthorn (JS), and three Holstein (HO) cattle (determined in this study), bovine control (GenBank accession no. U15969), and Hereford (HE) cattle (AAFC03111659). For each FGF4, a period indicates sequence identity to FGF4 from JB, JS and HO cattle. A dash represents a gap introduced to optimize the alignment. The nucleotide sequence of the structural gene for HE was partially determined, and unidentified regions are indicated as blanks and amino acid positions are indicated in accordance with the partial sequences. An arrowhead indicates a possible processing site estimated from that of human FGF4 (Delli-Bovi *et al.* 1988).

sequences were identified, such as observed in one HO cow (AB633205) showing an insertion of GC nucleotides after position 613 (numbers indicate positions from the adenine base in the initiation codon) and one JS cow (AB633211) showing a G770T mutation. Because sample sizes were small in the respective breeds examined, it was still unknown whether the differences in nucleotide sequences for introns of the *FGF4* gene detected in this study were attributed to inter- or intra-breed differences.

In conclusion, nucleotide sequences of the structural gene encoding FGF4 protein were completely identical in all examined cattle derived from the three breeds. Therefore, we cannot rule out a possibility that this type of structural gene is widely distributed in cattle. To the best of our knowledge, this is the first determination of the complete nucleotide sequence in identified breeds.

ACKNOWLEDGMENTS

We thank Kazuhiro Rikimaru (Livestock Experiment Station, Akita Prefectural Agriculture, Forestry and Fisheries Research Center, Daisen, Japan) for invaluable comments on the manuscript. This work was supported in part by a research grant from the President of Akita Prefectural University to M. K.

REFERENCES

Amarnath D, Li X, Kato Y, Tsunoda Y. 2007. Gene expression in individual bovine somatic cell cloned embryos at the 8-cell and blastocyst stages of preimplantation development. *Journal of Reproduction and Development* **53,** 1247–1263.

Cibelli JB, Stice SL, Golueke PJ, Kane JJ, Jerry J, Blackwell C, Ponce de Leon FA, Robl JM. 1998. Cloned transgenic calves produced from nonquiescent fetal fibroblasts. *Science* **280,** 1256–1258.

Degrelle SA, Campion E, Cabau C, Piumi F, Reinaud P, Richard C, Renard JP, Hue I. 2005. Molecular evidence for a critical period in mural trophoblast development in bovine blastocysts. *Devevelopmental Biology* **288,** 448–460.

Delli-Bovi P, Curatola AM, Newman KM, Sato Y, Moscatelli D, Hewick RM, Rifkin DB, Basilico C. 1988. Processing, secretion, and biological properties of a novel growth factor of the fibroblast growth factor family with oncogenic potential. *Molecular and Cellular Biology* **8,** 2933–2941.

Feldman B, Poueymirou W, Papaioannou VE, DeChiara TM, Goldfarb M. 1995. Requirement of FGF-4 for postimplantation mouse development. *Science* **267,** 246–249.

Fujii T, Moriyasu S, Hirayama H, Hashizume T, Sawai K. 2010. Aberrant expression patterns of genes involved in segregation of inner cell mass and trophectoderm lineages in bovine embryos derived from somatic cell nuclear transfer. *Cellular Reprogramming* **12,** 617–625.

Kato Y, Tani T, Sotomaru Y, Kurokawa K, Kato J, Doguchi H, Yasue H, Tsunoda Y. 1998. Eight calves cloned from somatic cells of a single adult. *Science* **282,** 2095–2098.

Niswander L, Martin GR. 1992. Fgf-4 expression during gastrulation, myogenesis, limb and tooth development in the mouse. *Development* **114,** 755–768.

Rodriguez-Alvarez L, Cox J, Tovar H, Einspanier R, Castro FO. 2010. Changes in the expression of pluripotency-associated genes during preimplantation and peri-implantation stages in bovine cloned and in vitro produced embryos. *Zygote* **18,** 269–279.

Tanaka S, Kunath T, Hadjantonakis A, Nagy A, Rossant J. 1998. Promotion of trophoblast stem cell proliferation by FGF4. *Science* **282,** 2072–2075.

Yu JC, DeSeabra AJ, Wang LM, Fleming TP, Chedid M, Miki T, Heidaran MA. 1995. An unexpected transforming gene in calf-thymus carrier DNA: bovine hst. *Gene* **162,** 333–334.

Zimin AV, Delcher AL, Florea L, Kelley DR, Schatz MC, Puiu D, Hanrahan F, Pertea G, Van Tassell CP, Sonstegard TS, Marcais G, Roberts M, Subramanian P, Yorke JA, Salzberg SL. 2009. A whole-genome assembly of the domestic cow, *Bos taurus*. *Genome Biology* **10,** R42.

Reprod Med Biol (2011) 10:221–229
DOI 10.1007/s12522-011-0093-6

REVIEW ARTICLE

Physiological function of hyaluronan in mammalian oocyte maturation

Masaki Yokoo · Eimei Sato

Received: 23 February 2011 / Accepted: 2 June 2011 / Published online: 29 June 2011

Abstract Despite its structural simplicity, hyaluronan exhibits a broad spectrum of biological activities. Cumulus expansion observed during oocyte maturation in mammals is also induced by hyaluronan accumulation in cumulus–oocyte complexes. It has been demonstrated that this volumetric change in cumulus–oocyte complexes correlates with the progression of oocyte maturation. We have investigated the molecular mechanism of oocyte maturation in mammals, focusing on hyaluronan accumulation in cumulus–oocyte complexes during cumulus expansion. In this review, we describe the physiological function of hyaluronan, emphasizing the progression of oocyte maturation in mammals based on our previous findings.

Keywords CD44 · Cumulus expansion · Hyaluronan · Meiotic resumption · Oocyte

Introduction

In vitro maturation of human oocytes retrieved from antral ovarian follicles is a new option for assisted reproductive technology (ART). The major benefits of in vitro maturation, especially for polycystic ovarian syndrome patients, include avoiding the risk of ovarian hyperstimulation syndrome, reduced cost and less complicated treatment; however, the efficiency of current in vitro maturation techniques is suboptimal in terms of obtaining the number of mature oocytes. In addition, the quality of oocytes is poor after in vitro maturation, showing increased frequency of retarded cleavage and inhibited development. Thus, in vitro maturation of oocytes for ART in humans still leaves some room for improvement.

In mammals, the oocyte is surrounded by several layers of compacted cumulus cells, forming a cumulus–oocyte complex (COC). After the preovulatory gonadotropin surge, the oocyte recommences meiotic resumption, completes germinal vesicle breakdown (GVBD), and progresses to metaphase II before ovulation. During oocyte maturation, the COC expands dramatically; this phenomenon is termed cumulus expansion. This expanded matrix is critical for normal and efficient reproduction because it binds the oocyte and the cumulus cells together, and protects the oocyte from the proteolytic and mechanical stresses during ovulation. Moreover, cumulus expansion contributes to the success of oocyte fertilization by stabilizing the structure of the zona pellucida and by stimulating sperm activation and motility [1–3]. Because this volumetric change in the COC occurs not only in vivo but also in vitro maturation, the physiological significance of cumulus expansion is important in the study of the developmental competence of mammalian oocytes matured and fertilized in vitro [4–7]. We have investigated the molecular mechanism of oocyte maturation in mammals, with special emphasis on hyaluronan accumulation in COCs during cumulus expansion. The physiological function of hyaluronan during oocyte maturation is the focus of this review.

M. Yokoo (✉)
Laboratory of Animal Reproduction, Faculty of Bioresource Sciences, Akita Prefectural University, 2-2 Aza Minami Ogata Village, Minamiakita-gun, Ogata 010-0444, Japan
e-mail: myokoo@akita-pu.ac.jp

E. Sato
Laboratory of Animal Reproduction,
Graduate School of Agricultural Science,
Tohoku University, Sendai 981-8555, Japan

Hyaluronan synthesis during cumulus expansion

Hyaluronan is an unbranched polymer composed of repeating glucuronic acid and *N*-acetyl glucosamine disaccharide units. Unlike other glycosaminoglycans that form proteoglycans, hyaluronan is not linked to a core protein. Despite its structural simplicity, hyaluronan exhibits a broad spectrum of biological activities by interacting with hyaluronan-binding proteins. Hyaluronan is known as an important component of extracellular matrices and body fluids through its binding to other matrix molecules such as proteoglycans, thereby organizing the architecture and regulating the mechanical properties of tissues such as cartilage. Hyaluronan provides a highly hydrated environment that is favorable for actively growing, moving, and renewing cells and tissues. It can also activate many signaling events in cells, thereby influencing processes such as apoptosis, adhesion, proliferation, migration, and development of cell shape [8–11].

Cumulus expansion is reportedly also the result of synthesis and accumulation of hyaluronan around the cumulus cells [12–14]. The hyaluronan synthesis of COCs is critically dependent upon two signal events: (1) stimulation by follicle stimulating hormone/equine chorionic gonadotropin (FSH/eCG), and (2) paracrine signals secreted by the oocyte, termed the cumulus expansion-enabling factors (CEEFs). Hyaluronan is synthesized by hyaluronan synthase (HAS), which has been reported to exhibit 3 isoforms (HAS1, HAS2, and HAS3) [15]. Studies on mice, pigs, and cattle have demonstrated that HAS2 mRNA is strongly expressed in the cumulus cells stimulated by FSH/eCG, and that it controls cumulus expansion [16–18]. A transient increase of intercellular cyclic adenosine monophosphate (cAMP) is triggered by FSH treatment, and dbcAMP, a synthetic analog of cAMP, induces similar effects on hyaluronan synthesis, suggesting that FSH action is mediated by this cyclic nucleotide [19, 20]. In addition to FSH/eCG stimulation, expansion of the COC requires an oocyte-secreted paracrine signal. Studies in vitro have also shown that cumulus cells dissected from mouse COCs and cultured without oocytes do not produce significantly higher amounts of hyaluronan when stimulated with FSH but do so when oocytes or oocyte-conditioned medium are present [12]. In mice, the oocyte-specific member of the transforming growth factor-beta superfamily, growth differentiation factor-9 (GDF-9) and bone morphogenetic protein-15 (BMP-15) also promote cumulus expansion, suggesting that GDF-9 and/or BMP-15 are CEEFs [21–23]. Thus, synthesis of hyaluronan by mouse cumulus cells requires the combined action of FSH/eCG and CEEFs produced by the oocyte. On the other hand, pig, bovine, and rat oocytes all produce CEEF because they enable the FSH-stimulated expansion of mouse oocytectomized complexes. Nevertheless, the oocyte does not need to be present at the time of cumulus expansion [24–26]; hence, the absolute requirement for the CEEF for cumulus expansion to proceed may be restricted to the mouse.

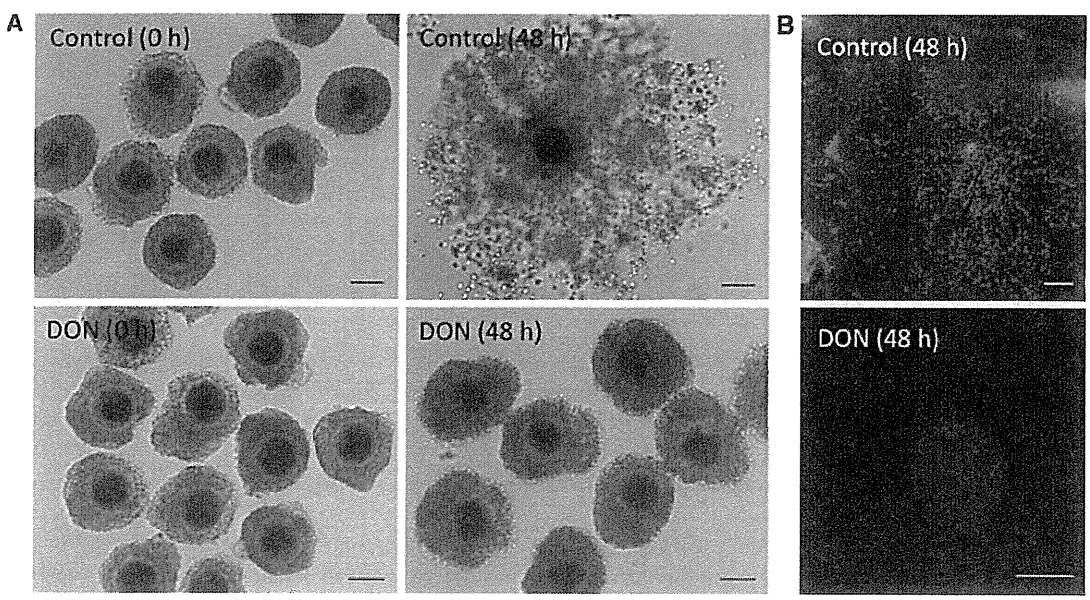

Fig. 1 Accumulation of hyaluronan in cumulus-oocyte complexes (COCs) during cumulus expansion. **a** Morphological observation of cumulus expansion in COCs during in vitro maturation with or without 6-diazo-5-oxo-l-norleucine (DON). **b** Localization of hyaluronan in porcine COCs as detected by immunofluorescence by using biotinylated hyaluronan-binding protein. *Bars* 100 μm

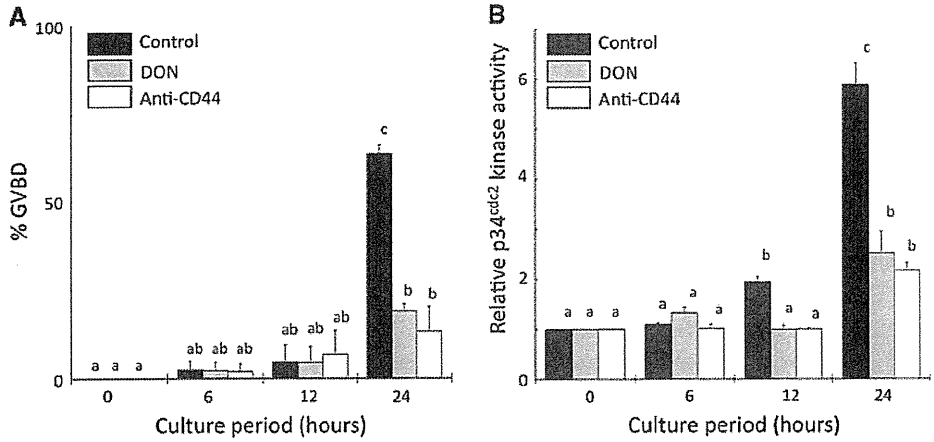

Fig. 2 Effects of hyaluronan–CD44 interaction on meiotic resumption. **a** Effects of 6-diazo-5-oxo-L-norleucine (DON) and anti-CD44 antibody on germinal vesicle breakdown (GVBD) in porcine oocytes. Cumulus-oocyte complexes (COCs) were cultured for up to 24 h in 1.0 mM DON or 5.0 μg/mL anti-CD44 antibody. **b** Effects of DON and anti-CD44 antibody on $p34^{cdc2}$ kinase activity in porcine oocytes. COCs were cultured for up to 24 h in 1.0 mM DON or 5.0 μg/mL anti-CD44 antibody. Data are expressed as fold strength of $p34^{cdc2}$ kinase activity relative to the activity in oocytes immediately after collection from follicles (0-h culture), which was set at a value of 1. *Lowercase letters* denote significant differences ($p < 0.05$). Data represent the mean ± SEM

We also observed a remarkable accumulation of hyaluronan in porcine-expanded COCs by immunostaining, but hyaluronan accumulation was completely inhibited by treatment with 6-diazo-5-oxo-1-norleucine (DON) (an inhibitor of hyaluronan synthesis) (Fig. 1) [27]. These results show that cumulus expansion of COCs is dependent on hyaluronan synthesis and accumulation. Moreover, we demonstrated that inhibition of cumulus expansion by DON resulted in a decrease in the rate of oocyte maturation in a dose-dependent manner. These results imply that hyaluronan accumulation is not only involved in the expansion of COC volume but also in the induction of oocyte maturation. The most recent studies indicated that inhibition of cumulus expansion by DON inhibited the activation of maturation promoting factor (MPF) and GVBD of the oocytes (Fig. 2) [28]. In summary, these data imply that hyaluronan synthesis during cumulus expansion plays an important role in the progression of meiotic resumption.

Hyaluronan-associated proteins on cumulus expansion

Hyaluronan synthesis is not sufficient for organizing an extracellular matrix. In general, hyaluronan needs extracellular hyaluronan-associated protein(s), an important subset of proteins with highly homologous sequences for hyaluronan binding, to organize the hyaluronan-rich matrix [29]. It has been reported that three proteins have been identified as essential for proper formation and stability of the hyaluronan matrix of COCs: inter-α-trypsin inhibitor (ITI), tumor necrosis factor-induced protein 6 (TSG6), and pentraxin 3 (PTX3) [14, 30, 31].

The ITI family isolated from serum reportedly plays an important role in the formation of the extracellular matrix, of which hyaluronan is a predominant component [32]. Proteins of the ITI family are composed of a common light chain called bikunin and 1 or 2 heavy polypeptide chains (HCs). The hyaluronan–HC complex is found in the hyaluronan-rich matrix of expanded COCs; hyaluronan covalently binds to the HCs released by the proteins of the ITI family during cumulus expansion [14, 33, 34]. Moreover, in bikunin-null mice, COCs exhibited defective formation of extracellular hyaluronan-rich matrix because of impaired synthesis of the ITI family proteins, and the mice developed severe infertility [14]. TSG6 is synthesized by cumulus cells and mural granulose cells of antral follicles after the gonadotropin surges. This protein has the ability to specifically bind to hyaluronan and to interact with the ITI family and the HCs of the ITI family are covalently transferred to hyaluronan by catalysis of TSG6 [35]. PTX3 synthesis also increases in mouse and human cumulus cells during the time preceding ovulation and localizes in the COC extracellular matrix [30, 31]. Although PTX3 does not bind to hyaluronan, the N-terminal domain of PTX3 interacts with the HCs of the ITI family and this portion of the molecule is necessary and sufficient for organizing hyaluronan and for enabling matrix formation of the COCs [36]. Both TSG6- and PTX3-deficient mice synthesize a normal amount of HAS2 expression, but they are infertile due to their inability to organize hyaluronan into a stable matrix [31, 37]. Although it is not clear whether these hyaluronan-associated proteins affect the progression of oocyte maturation, these reports suggest that these proteins may modulate the hyaluronan function during cumulus expansion.

Hyaluronan receptor (CD44) on cumulus expansion

CD44 is the most studied cell–surface receptor for hyaluronan and is present in a number of isoforms with different molecular sizes in a wide variety of cell types [38–41]. It is a transmembrane protein consisting of extracellular and cytoplasmic domains linked through transmembrane segments in the cell membranes of a variety of cells [42]. The form and function of CD44 can change depending on the cell type. CD44 expression has also been found in COCs during oocyte maturation [16, 43–45]. Immunoblotting analysis revealed that a single band of CD44 was detected between 85 and 90 kDa in COCs and the increase in its expansion was dependent on the degree of cumulus expansion [45]. The expression of CD44 in COCs appears to be controlled by FSH/eCG stimulation [16].

Moreover, when COCs were cultured with anti-CD44 antibody, oocyte maturation was inhibited in an antibody concentration-dependent manner, which had a blocking effect on the hyaluronan-binding ability of CD44 [46–49]. The most recent results indicated that the binding between hyaluronan and CD44 during cumulus expansion is highly significant for MPF activity and meiotic resumption of the oocytes (Fig. 2) [28]. Interestingly, this antibody does not affect the degree of cumulus expansion. Although previous studies have reported that the physiological significance of cumulus expansion is oocyte maturation, these results indicate that cumulus expansion is a necessary condition for oocyte maturation; however, cumulus expansion only is insufficient [50]. The results of these studies suggest that sufficient interaction between hyaluronan and CD44 is essential for meiotic resumption of the oocytes.

Function of hyaluronan in meiotic resumption

We demonstrated that hyaluronan played an important role in meiotic resumption of oocytes via CD44; however, because CD44 was expressed in cumulus cells and not in oocytes [45, 49], details of the mechanism by which hyaluronan regulates the progression of meiotic resumption has remained unclear. The critical component of meiotic resumption is MPF, a serine/threonine protein kinase composed of a regulatory unit, cyclin B, and a catalytic subunit, $p34^{cdc2}$ [51, 52]. In mammals, MPF activation is controlled by the concentration of cAMP in the oocyte. cAMP is synthesized in the cumulus cells and transferred into the oocytes via gap junctions in the COCs. Therefore, meiotic resumption of oocytes is regulated by gap junctional communication between the oocyte and the cumulus cells following the preovulatory gonadotropin surges. Therefore, we hypothesized that the effects of hyaluronan on oocyte maturation are related to the mechanism of gap junction gating in COCs. Connexin 43 (Cx43) is the most abundant gap junction protein; it is expressed by the ovarian follicles of many species [53–56] and also expressed in COCs as phosphorylated forms (Fig. 3a, b). We evaluated the effects of hyaluronan–CD44 interaction on the expression of Cx43. The results showed that exposure of COCs to DON or anti-CD44 antibody from 24 to

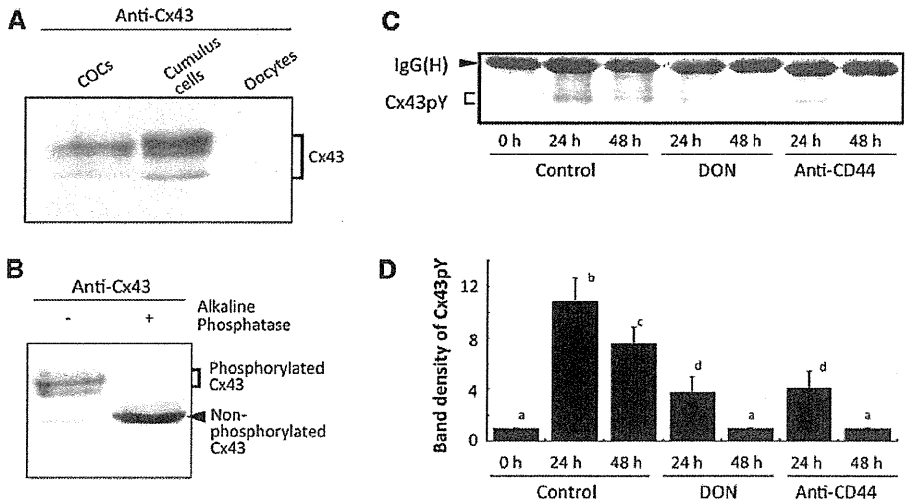

Fig. 3 Immunoblotting analysis of connexin 43 (Cx43) in cumulus–oocyte complexes (COCs). **a** Extracts of COCs, cumulus cells, and denuded oocytes were analyzed by immunoblotting with anti-Cx43 antibody. **b** Two samples of cultured COCs were treated with or without alkaline phosphatase. At the end of the treatment, the samples were subjected to immunoblotting analysis with anti-Cx43 antibody. **c** Detection of tyrosine-phosphorylated Cx43 (Cx43pY). The extracts immunoprecipitated with anti-Cx43 antibody were probed with anti-phosphotyrosine antibody. The *arrowhead* indicates the immunoglobulin heavy chain band (IgG (H)). **d** Densitometric analysis of (**c**). *Different superscripts* denote significant differences ($p < 0.05$). Data represent mean ± SD

48 h of incubation had no effect on the expression of total Cx43. Conversely, these treatments significantly inhibited the tyrosine phosphorylation of Cx43 in COCs (Fig. 3c, d) [57]. A previous study showed that Cx43 is phosphorylated at multiple residues, and that gap junction function is regulated by several kinases [58, 59]. The closure of Cx43-containing gap junctions is induced by phosphorylation of this protein on the tyrosines at positions 247 and 265 [60–62]. Therefore, our results revealed that hyaluronan induced the closure of Cx43-containing gap junctions in COCs via tyrosine phosphorylation, and meiotic resumption subsequently occurred in the oocytes. Previous studies showed that Src tyrosine kinase induces tyrosine phosphorylation of Cx43 and inhibits intercellular gap junctional communication [61–65]. In addition, the interaction between hyaluronan and CD44 has been shown to stimulate the activation of tyrosine kinases such as Src kinase [66–68]. Although the function of Src kinase in the cumulus cells during oocyte maturation is unclear, we speculate that hyaluronan induces the tyrosine phosphorylation of Cx43 via Src kinase.

Interestingly, we observed these results using a maturation medium without luteinizing hormone (LH). Several previous studies have demonstrated that LH is a key factor in the initiation of oocyte maturation in vivo and in vitro, and it is involved in the regulation of closure of the Cx43-containing gap junctions in COCs. Various studies have investigated the signal transduction pathway and LH-stimulated maturational processes. Cx43 levels are reduced in response to the preovulatory surge of LH [69, 70]. In addition, LH stimulates the phosphorylation of this gap junction protein [59, 71, 72]. Recent studies showed that LH causes mitogen-activated protein kinase-dependent serine phosphorylation and closure of Cx43-containing gap junctions, allowing meiotic resumption [73]. In addition, it has been shown that progesterone induces reduction in Cx43 expression via the progesterone receptor, which is induced by stimulation with LH, also resulting in meiotic resumption [74]. Moreover, the LH-induced decrease in Cx43 permeability is reportedly not due to phosphorylation at tyrosine sites [75, 76]. Considering that hyaluronan induces tyrosine phosphorylation of Cx43, the meiosis stimulatory function of hyaluronan is likely to be independent of the meiosis stimulatory pathway of LH. The relationship between hyaluronan and LH with regard to meiotic resumption of the oocytes is undocumented and needs to be addressed.

Hyaluronan-binding ability of CD44 and oocyte maturation

In general, oocytes that have matured in vitro have a reduced capacity to be fertilized and a higher rate of abnormal fertilization and development as compared to their in vivo counterparts. Although oocytes that have matured in vitro can be penetrated by spermatozoa under appropriate conditions, in vitro maturation is associated with low rates of pronuclear formation and a high incidence of polyspermy [77]. Furthermore, the rate of embryo development of in vitro-matured and fertilized COCs is significantly lower than that observed in vivo [78]. The results of our experiments suggest that the binding between hyaluronan and CD44 during cumulus expansion is important for oocyte maturation. Therefore, we focused on the role of the CD44 molecule in cumulus expansion for the in vitro and in vivo comparisons in our study [49, 79]. Immunoblotting analysis indicated a difference in the size of CD44 between the in vivo and in vitro samples. While the CD44 band of the in vitro-matured COCs was 81–88 kDa in size, the CD44 band of the in vivo-matured COCs was 73–83 kDa in size. Sialidase treatment reduced the size of the CD44 obtained from the COCs matured in vitro to a size similar to that of the CD44 from the COCs matured in vivo. These results suggest that during cumulus expansion, the CD44 in the in vitro-matured COCs contains more sialic acids than the CD44 in the in vivo-matured COCs. The extracellular domain of CD44 reportedly contains the necessary motifs for binding hyaluronan [80], and glycosylation of its extracellular domain has been implicated in the regulation of the hyaluronan-binding ability of CD44 [39]. In particular, enzymatic hydrolysis of sialic acid molecules augments the ability to bind hyaluronan, implying that the terminal sialic acids of CD44 have an inhibitory effect on the hyaluronan-binding ability of CD44 [81–83]. Although we did not measure the ability of CD44 to bind hyaluronan, our results indicated the possibility that the interaction between hyaluronan and CD44 during in vitro maturation may not be sufficient for oocyte maturation compared to in vivo maturation. Based on these observations, we speculate that insufficient interaction of hyaluronan with CD44 during in vitro maturation may cause inferior fertilization and developmental capacity in the oocytes compared to those matured in vivo. These results may represent a new target for controlling oocyte maturation and oocyte quality in the in vitro culture systems.

Concluding remarks

In conclusion, we propose a model wherein hyaluronan serves a previously unrecognized role in inducing meiotic resumption (Fig. 4). Hyaluronan secreted from the cumulus cells is synthesized by HAS2, whose level of expression is controlled by FSH/eCG. Hyaluronan secreted from the cumulus cells is linked to the hyaluronan-associated proteins (ITI, TSG6 and PTX3) and forms an hyaluronan-rich

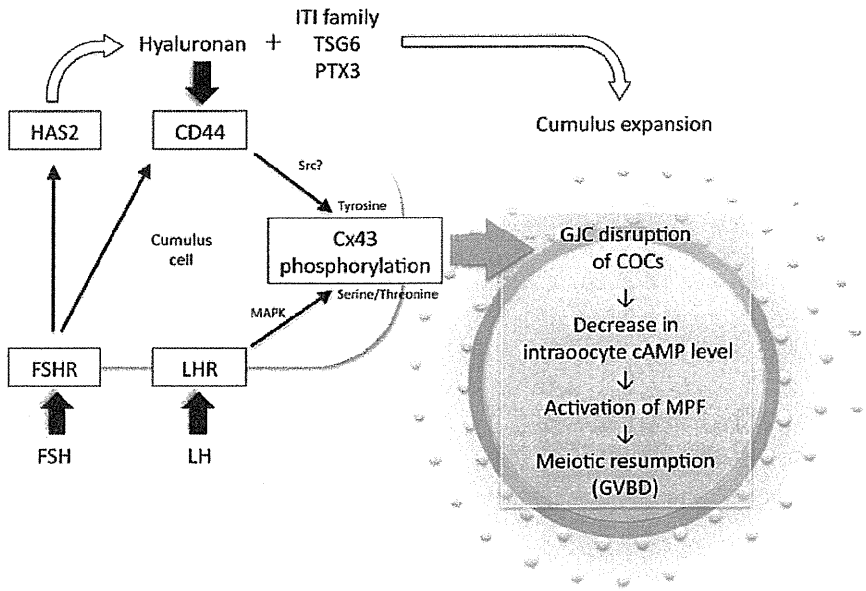

Fig. 4 A proposed model for hyaluronan-induced mammalian oocyte meiotic resumption. *FSH* follicle-stimulating hormone, *LH* luteinizing hormone, *FSHR* FSH receptor, *LHR* LH receptor, *HAS2* hyaluronan synthase 2, *ITI* inter-α-trypsin inhibitor, *TSG6* tumor necrosis factor-induced protein 6, *PTX3* pentraxin 3, *Cx43* connexin 43, *MAPK* mitogen-activated protein kinase, *GJC* gap junctional communication, *cAMP* cyclic adenosine 3′,5′-monophosphate, *MPF* maturation promoting factor, *GVBD* germinal vesicle breakdown

matrix in the COCs, resulting in cumulus expansion. FSH/eCG stimulation also results in the expression of hyaluronan receptor CD44 on cumulus cells. The hyaluronan accumulated during cumulus expansion binds to CD44 and induces the phosphorylation of Cx43 at tyrosine residues. The hyaluronan–CD44 interaction during cumulus expansion induces disruption of the gap junctional communication in the COCs, inhibits the transport of cAMP from the cumulus cells into the oocytes, and leads to MPF activation and meiotic resumption of oocytes. On the other hand, LH also induces meiotic resumption of the oocytes, and it is quite likely that LH interrupts the gap junctional communication in the COCs by another pathway involving hyaluronan.

Our studies provide the evidence that the hyaluronan–CD44 interaction during cumulus expansion of COCs acts to induce the progression of meiotic resumption in the oocytes. In mice, it is known that CD44 is not essential to induce the ovulation process and that CD44 mutant mice are fertile; however, it is also known that spontaneous maturation occurs in mouse oocytes and that a normal percentage develop to live offspring when fertilization does occur in these oocytes [84]. Thus, the function of the hyaluronan–CD44 interaction may be not necessarily essential for mouse oocyte maturation that is not critically dependent on gonadotropin. Although the dependence of the hyaluronan–CD44 interaction on the oocyte maturation process in other species is poorly understand, we speculate that the gonadotropin-induced meiotic resumption process of mammalian oocytes requires sufficient interaction between hyaluronan and CD44 during cumulus expansion. In vitro maturation of oocytes for ART in humans has not yet been completely established. In particular, cumulus expansion during in vitro maturation of human COCs has failed. We hope that this review will lead to an improvement in the in vitro oocyte maturation techniques for ART.

Acknowledgments This review was based on the findings of our previous studies. The authors thank all of the members in the laboratory of animal reproduction of Tohoku University for their helpful support and discussion.

References

1. Meizel S. Molecules that initiate or help stimulate the acrosome reaction by their interaction with the mammalian sperm surface. Am J Anat. 1985;174:285–302.
2. Huszar G, Willetts M, Corrales M. Hyaluronic acid (sperm select) improves retention of sperm motility and velocity in normospermic and oligospermic specimens. Fertil Steril. 1990;54:1127–34.
3. Kornovski BS, McCoshen J, Kredentser J, Turley E. The regulation of sperm motility by a novel hyaluronan receptor. Fertil Steril. 1994;61:935–40.
4. Chen L, Russell PT, Larsen WJ. Functional significance of cumulus expansion in the mouse: roles for the preovulatory synthesis of hyaluronic acid within the cumulus mass. Mol Reprod Dev. 1993;34:87–93.
5. Ball GD, Leibfried ML, Lenz RW, Ax RL, Bavister BD, First NL. Factors affecting successful in vitro fertilization of bovine follicular oocytes. Biol Reprod. 1983;28:717–25.
6. Yang LS, Kadam AL, Koide SS. Identification of a cAMP-dependent protein kinase in bovine and human follicular fluids. Biochem Mol Biol Int. 1993;31:521–5.
7. Qian Y, Shi WQ, Ding JT, Sha JH, Fan BQ. Predictive value of the area of expanded cumulus mass on development of porcine oocytes matured and fertilized in vitro. J Reprod Dev. 2003;49:167–74.
8. Thorne RF, Legg JW, Isacke CM. The role of the CD44 transmembrane and cytoplasmic domains in co-ordinating adhesive and signalling events. J Cell Sci. 2004;117:373–80.

9. Misra S, Obeid LM, Hannun YA, Minamisawa S, Berger FG, Markwald RR, et al. Hyaluronan constitutively regulates activation of COX-2-mediated cell survival activity in intestinal epithelial and colon carcinoma cells. J Biol Chem. 2008;283: 14335–44.
10. Turley EA, Noble PW, Bourguignon LY. Signaling properties of hyaluronan receptors. J Biol Chem. 2002;277:4589–92.
11. Toole BP, Slomiany MG. Hyaluronan: a constitutive regulator of chemoresistance and malignancy in cancer cells. Semin Cancer Biol. 2008;18:244–50.
12. Salustri A, Yanagishita M, Hascall VC. Mouse oocytes regulate hyaluronic acid synthesis and mucification by FSH-stimulated cumulus cells. Dev Biol. 1990;138:26–32.
13. Chen L, Wert SE, Hendrix EM, Russell PT, Cannon M, Larsen WJ. Hyaluronic acid synthesis and gap junction endocytosis are necessary for normal expansion of the cumulus mass. Mol Reprod Dev. 1990;26:236–47.
14. Zhuo L, Yoneda M, Zhao M, Yingsung W, Yoshida N, Kitagawa Y, et al. Defect in SHAP-hyaluronan complex causes severe female infertility. A study by inactivation of the bikunin gene in mice. J Biol Chem. 2001;276:7693–6.
15. Spicer AP, McDonald JA. Characterization and molecular evolution of a vertebrate hyaluronan synthase gene family. J Biol Chem. 1998;273:1923–32.
16. Kimura N, Konno Y, Miyoshi K, Matsumoto H, Sato E. Expression of hyaluronan synthases and CD44 messenger RNAs in porcine cumulus-oocyte complexes during in vitro maturation. Biol Reprod. 2002;66:707–17.
17. Schoenfelder M, Einspanier R. Expression of hyaluronan synthases and corresponding hyaluronan receptors is differentially regulated during oocyte maturation in cattle. Biol Reprod. 2003;69:269–77.
18. Fulop C, Salustri A, Hascall VC. Coding sequence of a hyaluronan synthase homologue expressed during expansion of the mouse cumulus-oocyte complex. Arch Biochem Biophys. 1997; 337:261–6.
19. Salustri A, Petrungaro S, De Felici M, Conti M, Siracusa G. Effect of follicle-stimulating hormone on cyclic adenosine monophosphate level and on meiotic maturation in mouse cumulus cell-enclosed oocytes cultured in vitro. Biol Reprod. 1985;33:797–802.
20. Salustri A, Yanagishita M, Hascall VC. Synthesis and accumulation of hyaluronic acid and proteoglycans in the mouse cumulus cell-oocyte complex during follicle-stimulating hormone-induced mucification. J Biol Chem. 1989;264:13840–7.
21. Dragovic RA, Ritter LJ, Schulz SJ, Amato F, Armstrong DT, Gilchrist RB. Role of oocyte-secreted growth differentiation factor 9 in the regulation of mouse cumulus expansion. Endocrinology. 2005;146:2798–806.
22. Gueripel X, Brun V, Gougeon A. Oocyte bone morphogenetic protein 15, but not growth differentiation factor 9, is increased during gonadotropin-induced follicular development in the immature mouse and is associated with cumulus oophorus expansion. Biol Reprod. 2006;75:836–43.
23. Yoshino O, McMahon HE, Sharma S, Shimasaki S. A unique preovulatory expression pattern plays a key role in the physiological functions of BMP-15 in the mouse. Proc Natl Acad Sci USA. 2006;103:10678–83.
24. Ralph JH, Telfer EE, Wilmut I. Bovine cumulus cell expansion does not depend on the presence of an oocyte secreted factor. Mol Reprod Dev. 1995;42:248–53.
25. Prochazka R, Nemcova L, Nagyova E, Kanka J. Expression of growth differentiation factor 9 messenger RNA in porcine growing and preovulatory ovarian follicles. Biol Reprod. 2004; 71:1290–5.
26. Vanderhyden BC. Species differences in the regulation of cumulus expansion by an oocyte-secreted factor(s). J Reprod Fertil. 1993;98:219–27.
27. Yokoo M, Kimura N, Abe H, Sato E. Influence of hyaluronan accumulation during cumulus expansion on in vitro porcine oocyte maturation. Zygote. 2008;16:309–14.
28. Yokoo M, Kimura N, Sato E. Induction of oocyte maturation by hyaluronan-CD44 interaction in pigs. J Reprod Dev. 2010;56: 15–9.
29. Laurent TC, Fraser JR. Hyaluronan. Faseb J. 1992;6:2397–404.
30. Varani S, Elvin JA, Yan C, DeMayo J, DeMayo FJ, Horton HF, et al. Knockout of pentraxin 3, a downstream target of growth differentiation factor-9, causes female subfertility. Mol Endocrinol. 2002;16:1154–67.
31. Salustri A, Garlanda C, Hirsch E, De Acetis M, Maccagno A, Bottazzi B, et al. PTX3 plays a key role in the organization of the cumulus oophorus extracellular matrix and in in vivo fertilization. Development. 2004;131:1577–86.
32. Enghild JJ, Salvesen G, Hefta SA, Thogersen IB, Rutherfurd S, Pizzo SV. Chondroitin 4-sulfate covalently cross-links the chains of the human blood protein pre-alpha-inhibitor. J Biol Chem. 1991;266:747–51.
33. Chen L, Zhang H, Powers RW, Russell PT, Larsen WJ. Covalent linkage between proteins of the inter-alpha-inhibitor family and hyaluronic acid is mediated by a factor produced by granulosa cells. J Biol Chem. 1996;271:19409–14.
34. Nagyova E, Camaioni A, Prochazka R, Salustri A. Covalent transfer of heavy chains of inter-alpha-trypsin inhibitor family proteins to hyaluronan in in vivo and in vitro expanded porcine oocyte-cumulus complexes. Biol Reprod. 2004;71:1838–43.
35. Rugg MS, Willis AC, Mukhopadhyay D, Hascall VC, Fries E, Fulop C, et al. Characterization of complexes formed between TSG-6 and inter-alpha-inhibitor that act as intermediates in the covalent transfer of heavy chains onto hyaluronan. J Biol Chem. 2005;280:25674–86.
36. Scarchilli L, Camaioni A, Bottazzi B, Negri V, Doni A, Deban L, et al. PTX3 interacts with inter-alpha-trypsin inhibitor: implications for hyaluronan organization and cumulus oophorus expansion. J Biol Chem. 2007;282:30161–70.
37. Fulop C, Szanto S, Mukhopadhyay D, Bardos T, Kamath RV, Rugg MS, et al. Impaired cumulus mucification and female sterility in tumor necrosis factor-induced protein-6 deficient mice. Development. 2003;130:2253–61.
38. Aruffo A, Stamenkovic I, Melnick M, Underhill CB, Seed B. CD44 is the principal cell surface receptor for hyaluronate. Cell. 1990;61:1303–13.
39. Bartolazzi A, Nocks A, Aruffo A, Spring F, Stamenkovic I. Glycosylation of CD44 is implicated in CD44-mediated cell adhesion to hyaluronan. J Cell Biol. 1996;132:1199–208.
40. Lesley J, Hyman R, Kincade PW. CD44 and its interaction with extracellular matrix. Adv Immunol. 1993;54:271–335.
41. Underhill C. CD44: the hyaluronan receptor. J Cell Sci. 1992;103(Pt 2):293–8.
42. Bajorath J. Molecular organization, structural features, and ligand binding characteristics of CD44, a highly variable cell surface glycoprotein with multiple functions. Proteins. 2000;39:103–11.
43. Furnus CC, Valcarcel A, Dulout FN, Errecalde AL. The hyaluronic acid receptor (CD44) is expressed in bovine oocytes and early stage embryos. Theriogenology. 2003;60:1633–44.
44. Ohta N, Saito H, Kuzumaki T, Takahashi T, Ito MM, Saito T, et al. Expression of CD44 in human cumulus and mural granulosa cells of individual patients in in vitro fertilization programmes. Mol Hum Reprod. 1999;5:22–8.
45. Yokoo M, Miyahayashi Y, Naganuma T, Kimura N, Sasada H, Sato E. Identification of hyaluronic acid-binding proteins and

their expressions in porcine cumulus-oocyte complexes during in vitro maturation. Biol Reprod. 2002;67:1165–71.
46. Peach RJ, Hollenbaugh D, Stamenkovic I, Aruffo A. Identification of hyaluronic acid binding sites in the extracellular domain of CD44. J Cell Biol. 1993;122:257–64.
47. Trowbridge IS, Lesley J, Schulte R, Hyman R, Trotter J. Biochemical characterization and cellular distribution of a polymorphic, murine cell-surface glycoprotein expressed on lymphoid tissues. Immunogenetics. 1982;15:299–312.
48. Zheng Z, Katoh S, He Q, Oritani K, Miyake K, Lesley J, et al. Monoclonal antibodies to CD44 and their influence on hyaluronan recognition. J Cell Biol. 1995;130:485–95.
49. Yokoo M, Tientha P, Kimura N, Niwa K, Sato E, Rodriguez-Martinez H. Localisation of the hyaluronan receptor CD44 in porcine cumulus cells during in vivo and in vitro maturation. Zygote. 2002;10:317–26.
50. Yokoo M, Shimizu T, Kimura N, Tunjung WA, Matsumoto H, Abe H, Sasada H, Rodriguez-Martinez H, Sato E. Role of the hyaluronan receptor CD44 during porcine oocyte maturation. J Reprod Dev. 2007;53:263–70.
51. Labbe JC, Picard A, Peaucellier G, Cavadore JC, Nurse P, Doree M. Purification of MPF from starfish: identification as the H1 histone kinase p34cdc2 and a possible mechanism for its periodic activation. Cell. 1989;57:253–63.
52. Lohka MJ, Hayes MK, Maller JL. Purification of maturation-promoting factor, an intracellular regulator of early mitotic events. Proc Natl Acad Sci USA. 1988;85:3009–13.
53. Shimada M, Maeda T, Terada T. Dynamic changes of connexin-43, gap junctional protein, in outer layers of cumulus cells are regulated by PKC and PI 3-kinase during meiotic resumption in porcine oocytes. Biol Reprod. 2001;64:1255–63.
54. Vozzi C, Formenton A, Chanson A, Senn A, Sahli R, Shaw P, et al. Involvement of connexin 43 in meiotic maturation of bovine oocytes. Reproduction. 2001;122:619–28.
55. Valdimarsson G, De Sousa PA, Kidder GM. Coexpression of gap junction proteins in the cumulus-oocyte complex. Mol Reprod Dev. 1993;36:7–15.
56. Sasseville M, Gagnon MC, Guillemette C, Sullivan R, Gilchrist RB, Richard FJ. Regulation of gap junctions in porcine cumulus-oocyte complexes: contributions of granulosa cell contact, gonadotropins, and lipid rafts. Mol Endocrinol. 2009;23:700–10.
57. Yokoo M, Sato E. Cumulus-oocyte complex interactions during oocyte maturation. Int Rev Cytol. 2004;235:251–91.
58. Beyer EC, Kistler J, Paul DL, Goodenough DA. Antisera directed against connexin43 peptides react with a 43-kD protein localized to gap junctions in myocardium and other tissues. J Cell Biol. 1989;108:595–605.
59. Granot I, Dekel N. Phosphorylation and expression of connexin-43 ovarian gap junction protein are regulated by luteinizing hormone. J Biol Chem. 1994;269:30502–9.
60. Swenson KI, Piwnica-Worms H, McNamee H, Paul DL. Tyrosine phosphorylation of the gap junction protein connexin43 is required for the pp60v-src-induced inhibition of communication. Cell Regul. 1990;1:989–1002.
61. Lin R, Warn-Cramer BJ, Kurata WE, Lau AF. v-Src phosphorylation of connexin 43 on Tyr247 and Tyr265 disrupts gap junctional communication. J Cell Biol. 2001;154:815–27.
62. Kanemitsu MY, Loo LW, Simon S, Lau AF, Eckhart W. Tyrosine phosphorylation of connexin 43 by v-Src is mediated by SH2 and SH3 domain interactions. J Biol Chem. 1997;272:22824–31.
63. Azarnia R, Reddy S, Kmiecik TE, Shalloway D, Loewenstein WR. The cellular src gene product regulates junctional cell-to-cell communication. Science. 1988;239:398–401.
64. Crow DS, Beyer EC, Paul DL, Kobe SS, Lau AF. Phosphorylation of connexin43 gap junction protein in uninfected and Rous sarcoma virus-transformed mammalian fibroblasts. Mol Cell Biol. 1990;10:1754–63.
65. Filson AJ, Azarnia R, Beyer EC, Loewenstein WR, Brugge JS. Tyrosine phosphorylation of a gap junction protein correlates with inhibition of cell-to-cell communication. Cell Growth Differ. 1990;1:661–8.
66. Bourguignon LY, Zhu H, Shao L, Chen YW. CD44 interaction with c-Src kinase promotes cortactin-mediated cytoskeleton function and hyaluronic acid-dependent ovarian tumor cell migration. J Biol Chem. 2001;276:7327–36.
67. Fujita Y, Kitagawa M, Nakamura S, Azuma K, Ishii G, Higashi M, et al. CD44 signaling through focal adhesion kinase and its anti-apoptotic effect. FEBS Lett. 2002;528:101–8.
68. Murai T, Miyazaki Y, Nishinakamura H, Sugahara KN, Miyauchi T, Sako Y, et al. Engagement of CD44 promotes Rac activation and CD44 cleavage during tumor cell migration. J Biol Chem. 2004;279:4541–50.
69. Granot I, Dekel N. Developmental expression and regulation of the gap junction protein and transcript in rat ovaries. Mol Reprod Dev. 1997;47:231–9.
70. Wiesen JF, Midgley AR Jr. Changes in expression of connexin 43 gap junction messenger ribonucleic acid and protein during ovarian follicular growth. Endocrinology. 1993;133:741–6.
71. Kalma Y, Granot I, Galiani D, Barash A, Dekel N. Luteinizing hormone-induced connexin 43 down-regulation: inhibition of translation. Endocrinology. 2004;145:1617–24.
72. Sela-Abramovich S, Chorev E, Galiani D, Dekel N. Mitogen-activated protein kinase mediates luteinizing hormone-induced breakdown of communication and oocyte maturation in rat ovarian follicles. Endocrinology. 2005;146:1236–44.
73. Norris RP, Ratzan WJ, Freudzon M, Mehlmann LM, Krall J, Movsesian MA, et al. Cyclic GMP from the surrounding somatic cells regulates cyclic AMP and meiosis in the mouse oocyte. Development. 2009;136:1869–78.
74. Shimada M, Yamashita Y, Ito J, Okazaki T, Kawahata K, Nishibori M. Expression of two progesterone receptor isoforms in cumulus cells and their roles during meiotic resumption of porcine oocytes. J Mol Endocrinol. 2004;33:209–25.
75. Solan JL, Marquez-Rosado L, Sorgen PL, Thornton PJ, Gafken PR, Lampe PD. Phosphorylation at S365 is a gatekeeper event that changes the structure of Cx43 and prevents down-regulation by PKC. J Cell Biol. 2007;179:1301–9.
76. Solan JL, Lampe PD. Connexin 43 in LA-25 cells with active v-src is phosphorylated on Y247, Y265, S262, S279/282, and S368 via multiple signaling pathways. Cell Commun Adhes. 2008;15:75–84.
77. Hunter MG. Oocyte maturation and ovum quality in pigs. Rev Reprod. 2000;5:122–30.
78. Sun QY, Lai L, Bonk A, Prather RS, Schatten H. Cytoplasmic changes in relation to nuclear maturation and early embryo developmental potential of porcine oocytes: effects of gonadotropins, cumulus cells, follicular size, and protein synthesis inhibition. Mol Reprod Dev. 2001;59:192–8.
79. Tienthai P, Yokoo M, Kimura N, Heldin P, Sato E, Rodriguez-Martinez H. Immunohistochemical localization and expression of the hyaluronan receptor CD44 in the epithelium of the pig oviduct during oestrus. Reproduction. 2003;125:119–32.
80. Lesley J, Hyman R. CD44 structure and function. Front Biosci. 1998;3:d616–30.
81. Lesley J, English N, Perschl A, Gregoroff J, Hyman R. Variant cell lines selected for alterations in the function of the hyaluronan receptor CD44 show differences in glycosylation. J Exp Med. 1995;182:431–7.
82. Katoh S, Zheng Z, Oritani K, Shimozato T, Kincade PW. Glycosylation of CD44 negatively regulates its recognition of hyaluronan. J Exp Med. 1995;182:419–29.

83. Katoh S, Miyagi T, Taniguchi H, Matsubara Y, Kadota J, Tominaga A, et al. Cutting edge: an inducible sialidase regulates the hyaluronic acid binding ability of CD44-bearing human monocytes. J Immunol. 1999;162:5058–61.

84. Schroeder AC, Eppig JJ. The developmental capacity of mouse oocytes that matured spontaneously in vitro is normal. Dev Biol. 1984;102:493–7.

CELLULAR REPROGRAMMING
Volume 12, Number 4, 2010

DOI: 10.1089/cell.2009.0111

Anomalous Oxygen Consumption in Porcine Somatic Cell Nuclear Transfer Embryos

Satoshi Sugimura,[1,*] Masaki Yokoo,[2] Ken-ichi Yamanaka,[3] Manabu Kawahara,[4] Satoru Moriyasu,[5] Takuya Wakai,[6] Takashi Nagai,[7] Hiroyuki Abe,[8] and Eimei Sato[1]

Abstract

Oxygen consumption reflects overall metabolic activity of mammalian embryos. We measured oxygen consumption in individual porcine somatic cell nuclear transfer (SCNT) and *in vitro*-fertilized (IVF) embryos by modified scanning electrochemical microscopy. Oxygen consumption in IVF embryos rapidly increased at day 5 of the blastocyst stage (D5BL). IVF embryos that consumed $>0.81\times10^{14}$/mol sec^{-1} of oxygen at D5BL exhibited significantly higher hatching and hatched rates at D7BL, whereas D5BL SCNT embryos using porcine fetal fibroblasts did not show an increase in oxygen consumption until D7BL. The numbers of inner cell mass and trophectoderm (TE) cells and incidence of apoptosis did not significantly differ between IVF and SCNT embryos at D5BL. At D7BL, a significant lower number of TE cell and higher incidence of apoptosis were observed in SCNT than in IVF embryos; this significantly correlated with their oxygen consumption at D5BL. Use of cumulus cells as donor cells neutralized the low oxygen consumption in SCNT embryos at D5BL, regardless of the difference between the recipient cytoplasm and donor nucleus. Some of SCNT embryos at D7BL were retrieved the hatching completion and were improved the number of TE cell and apoptosis incidence by using cumulus cells. Thus, anomalous oxygen consumption in porcine SCNT embryos at D5BL could be sign of limited hatchability, which may be responsible for the low TE cell number and high apoptosis incidence.

Introduction

RECENTLY, THE *IN VITRO* BLASTOCYST FORMATION RATE has improved by advances in somatic cell nuclear transfer (SCNT) techniques such as treatment of recipient cytoplasts (Beebe et al., 2007; Kawahara et al., 2005; Wakai et al., 2008) and donor cells (Mohana Kumar et al., 2006), *in vitro* culture conditioning (Im et al., 2004; Yamanaka et al., 2009), activation (Yamanaka et al., 2007), and diploid complement retention with cytochalasin treatment (Sugimura et al., 2008). Nevertheless, the efficiency of cloning after embryo transfer still remains very low. To explore the underlying cause of low cloning efficiency, previous studies have performed global gene expression analysis using differential screening and cDNA microarray in SCNT embryos; the results of these studies revealed aberrant expression of genes associated with energy metabolism and mitochondrial function (Jincho et al., 2007; Vassena et al., 2007). Energy metabolism, including nutrient consumption, glycolysis, and oxidative phosphorylation, is crucial for cell proliferation and differentiation and embryo development and viability (Dumollard et al., 2007). Furthermore, in the *Xenopus* species, adenosine triphosphate (ATP)-dependent reactions have been suggested to affect the reprogramming of donor nuclei after SCNT (Kikyo et al., 2000). Thus, there have been some reports on physiological characteristics such as energy metabolism, including glucose uptake (Gao et al., 2003), glycolysis (Han et al., 2008), and ATP level (Boiani et al., 2004), in mouse SCNT embryos; however, energy metabolism in porcine SCNT embryos has not yet been elucidated.

[1]Laboratory of Animal Reproduction, Graduate School of Agricultural Science, Tohoku University, Sendai, Japan.
[2]Laboratory of Animal Reproduction, Faculty of Bioresource Sciences, Akita Prefectural University, Akita, Japan.
[3]National Agricultural Research Center for Kyushu Okinawa Region, Kumamoto, Japan.
[4]Laboratory of Animal Resource Development Faculty of Agriculture, Saga University, Saga, Japan.
[5]Hokkaido Animal Research Center, Shintoku, Japan.
[6]Department of Veterinary and Animal Sciences, University of Massachusetts, Amherst, Massachusetts.
[7]National Institute of Livestock and Grassland Science, Tsukuba 305-0901, Japan.
[8]Graduate School of Science and Engineering, Yamagata University, Yonezawa, Japan.
*Current address: National Livestock Breeding Center, Nishigo 961-8511, Japan.

In general, oxygen consumption is a good indicator of the overall metabolic activity of individual embryos because ATP is mostly generated by oxidative phosphorylation, a process in which oxygen plays a key role (Houghton et al., 1996; Leese, 2003; Thompson et al., 1996; Thompson, 2000; Trimarchi et al., 2000). Further, our previous studies have shown that oxygen consumption in individual *in vitro*-fertilized (IVF) bovine embryos directly correlated with the subsequent embryonic development (Abe and Hoshi, 2003; Shiku et al., 2001). These studies were performed using modified scanning electrochemical microscopy (SECM). The SECM system appears to be a reliable, noninvasive, and a highly sensitive method for the measurement of oxygen consumption in individual embryos (Shiku et al., 2001). In the present study, for a better understanding of the underlying cause of low cloning efficiency in pigs, we measured oxygen consumption by using SECM to evaluate energy metabolism in porcine SCNT embryos.

Materials and Methods

In vitro *maturation of oocytes*

Ovaries of prepubertal gilts from three-way crossing (Duroc boars×Landrace-Large White sows) were collected at a local slaughterhouse and transported to the laboratory within 2 h in a container containing warm saline. Porcine oocytes were aspirated from the antral follicles, 3 to 6 mm in diameter, using an 18-gauge needle attached to a 5-mL disposable syringe. Cumulus–oocyte complexes (COCs) with uniform ooplasm and compact cumulus cell mass were selected in modified Dulbecco's phosphate-buffered saline (PBS) medium containing 5.56 mM glucose (Wako, Osaka, Japan), 0.33 mM sodium pyruvate (Wako), 1% (v/v) antibiotic antimycotic solution (Sigma Chemical Co., St. Louis, MO, USA), and 4 mg/mL fatty acid-free bovine serum albumin (BSA; 128K7400, Sigma) (PB1) (Quinn et al., 1982). After washing in PB1, the COCs were cultured in BSA-free NCSU-23 medium (Miyoshi et al., 2000) for 44 h at 39°C in a highly humidified atmosphere of 5% CO_2 in air. COCs were sequentially cultured as described by Funahashi et al. (1993). For the first 22 h of maturation culture, the medium was supplemented with 10 IU/mL equine Chronic Gonadotropin (eCG; Serotropin; Teikokuzouki, Tokyo, Japan), 10 IU/mL human chorionic gonadotropin (hCG; Puberogen; Sankyo, Tokyo, Japan), 0.1 mg/mL cysteine (Sigma), 1 mM dibutyryl cyclic AMP (Sigma), and 10% (v/v) porcine follicular fluid. The culture for the subsequent 22 h was carried out in the same medium without eCG and hCG. After culturing, expanded cumulus cells of the COCs were removed by vortexing for 30 sec in PB1 containing 1 mg/mL hyaluronidase (Sigma), and the oocytes with the first polar body were selected as matured oocytes under a stereomicroscope, and they were transferred into PB1 and used for the experiments.

Donor cells

The present study was approved by the Ethics Committee for Care and Use of Laboratory Animals for Biomedical Research of the Graduate School of Agricultural Science, Tohoku University. Donor cells were isolated as described by Wakai et al. (2008). In brief, pig fetuses of Goettingen breed (CSK, Suwa, Japan) were collected from the sow on day 56 of pregnancy. Each fetus was decapitated and eviscerated. The remaining tissues were washed in PBS (Sigma) and then digested with 0.1% (w/v) trypsin-ethylenediaminetetraacetic acid (EDTA) (Sigma) for 45 min at 38.5°C. After digestion, the cells collected as porcine fetal fibroblast (pFF) cells were cultured in Dulbecco's modified Eagle medium (DMEM, Sigma) supplemented with 10% (v/v) fetal bovine serum (FBS; A51408X, Gemini Bio-Products, Chalabasas, CA, USA). The culture medium was replaced every 2 days until the cells reached confluence. Subsequently, the cells were harvested with 0.1% (w/v) trypsin in PBS containing 0.5 mM EDTA for 5 min at 38.5°C, frozen with a cryoprotectant (Cellbanker, Zenyaku, Tokyo, Japan) and stored in liquid nitrogen (passage 0). For an overall experiment, fetal fibroblasts derived from one female Goettingen breed were used (Wakai et al., 2008). However, in the only experiment for evaluating potential sex specific effects (Supplementary Table 1; see online supplementary material at www.liebertonline.com), we used male fetal fibroblasts from littermates with this female fetal fibroblasts. Prior to the start of experiments, the cells were thawed and cultured in DMEM plus 10% FBS and used between passages 4 and 9. The fibroblasts were cultured for 1 week after they had attained confluence and were then used as donor cells. As another type of donor cell to use, the porcine cumulus cells (pCC) were prepared. After *in vitro* culture of COCs for 44 h, cumulus cells were isolated from oocytes by pipetting in PB1 containing hyaluronidase. Then they were transferred to PB1 for use as donor cells. They were injected to enucleated oocytes either from the same female (pCC-Auto) or from a different female (pCC-Allo).

Through the experiments, donor cells were used pFF. We further used pCC in Experiments 6 and 7.

Nuclear transfer

We produced the SCNT embryos by the reconstruction of enucleated oocytes with somatic cells in accordance with previous work, in which we had already confirmed the reconstructed embryos to be survivable until adult nuclear transplant miniature pigs (Wakai et al., 2008). The cumulus-free oocytes were stained with 5 μg/mL Hoechst 33342 (Sigma) for 5 to 10 min at 39°C and transferred into PB1 containing 2.5 μg/mL cytochalasin D (Sigma). Enucleation was performed by aspirating the first polar body and a small volume of the adjacent cytoplasm with a enucleation pipette of 20 μm diameter using a piezo-driven unit (Primtech, Tokyo, Japan), and its success was confirmed by visualizing the presence of metaphase plates within the removed cytoplasm under ultraviolet (UV) light. The enucleated oocytes were washed three times with porcine zygote medium-3 (PZM-3) (Yoshioka et al., 2002) and transferred to a 100-μL droplet of PZM-3 for the subsequent microinjection or fusion of the donor nucleus. The donor cells were transferred to a 50 μL droplet of PB1. To produce SCNT embryos by microinjection of donor cells, their plasma membranes were broken by gently aspirating them in and out of the injection pipette of 10 μm in diameter before microinjection into cytoplasm. To produce SCNT embryos by the electric fusion, intact donor cells were

placed in the perivitelline space of recipient oocytes through the same slit in the zona pellucida that had been made for enucleation. Then they were fused with the recipient oocytes using LF 101 (TR Tech, Tokyo, Japan) by stimulating direct current pulses of 150 V/mm for 50 μsec in 0.28 M mannitol solution supplemented with 0.1 mM $MgSO_4$ and 0.01% (w/v) PVA (Yin et al., 2003). Throughout the experiments, nuclear transfer was performed by a microinjection method of donor cells into recipient cytoplasts. Only in Experiment 3 did we further perform the electrofusion method.

Activation and culture of SCNT embryos

The activation of embryos was performed as described by Yamanaka et al. (2007). In brief, to activate the SCNT embryos, the reconstructed embryos at 3 h after injection or fusion of donor cells were treated with 15 μM ionomycin (Sigma) in PZM-3 containing fatty acid-free BSA (Yoshioka et al., 2002) for 20 min at 38.5°C in 5% CO_2 in humidified air and then washed with PZM-3. Next, 20 SCNT embryos were cultured in a 100-μL droplet of PZM-3 containing 5 μg/mL cycloheximide (Sigma) with cytochalasin D (Sigma) for 5 h at 38.5°C in 5% CO_2 in humidified air and then washed five times with cycloheximide-free PZM-3 (Sugimura et al., 2008). Last, the 20 embryos were transferred to a 100-μL droplet of PZM-3 and cultured at 38.5°C in an atmosphere of 5% CO_2 in air.

In vitro *fertilization*

IVF was also performed with *in vitro*-matured (IVM) oocytes. After the IVM, oocytes were washed three times with fertilization medium (TU medium) (Miyoshi et al., 1999), and 30 to 40 oocytes were transferred to a 100-μL droplet of IVF medium. Cryopreserved semen from Duroc boars was thawed, and spermatozoa were washed twice by centrifugation (1000×*g* for 4 min) in Dulbecco's PBS supplemented with 1 mg/mL BSA. Spermatozoa were resuspended in IVF medium, and 20 to 30 μL of the suspension was added to the drop containing oocytes to give a final concentration of 3×10^5 cells/mL. At 6 h postinsemination, 20 oocytes were washed three times in 100 μL droplet of PZM-3 and cultured in 100 μL droplet of PZM-3 at 38.5°C in 5% CO_2 in air. In our laboratory IVF system using the boar sperm, the rate of penetration and normal fertilization (both male and female pronuclei and two polar bodies) was 95.1 and 61.5%, respectively (Yamanaka et al., 2009).

Collection of in vivo *produced embryos*

Protocol of "surgical collection of embryos" was according to manual on pig embryo transfer (Kashiwazaki, 1993). Day 160 to 220 prepubertal gilts (Large-White) were treated with 1500 IU eCG, followed 72 h later by 500 IU hCG. Artificial insemination (AI) was performed three times from 24 h after hCG. Embryos on day 4 and 5 (day 0 = the day of first AI) were recovered surgically from the gilts.

Production of parthenogenetically activated embryos

To generate different types of parthenogenetically activated embryos (PA), IVM porcine oocytes without manipulation were activated by using the same methods as those used for generating SCNT embryos. From these oocytes, a small volume of ooplasm was removed, and a minimal amount of PB1 medium was injected (Sham-PA); an enucleated pFF cell was also injected (SCI-PA) in these cells. Enucleation of pFF was performed using the method described by Hayashi et al. (1991) with slight modification. Upon reaching confluence, pFF cells were enucleated by centrifugation (23,000×*g* for 30 min) in DMEM with cytochalasin B (10 μg/mL) and Hoechst 33342. Enucleation was confirmed by visualizing the cells under UV light. Subsequently, plasma membranes of the cells, in which enucleation was confirmed, were disrupted by gently aspirating the cells in and out of the beveled pipette; their cytoplasts were injected into the oocytes.

Measurement of oxygen consumption

Oxygen consumption by individual porcine embryos was noninvasively measured by the SECM system (HV-405; Hokuto Denko Co., Tokyo, Japan) (Abe and Hoshi, 2003; Shiku et al., 2001). Embryos were transferred singularly to a plate filled with 5 mL of embryo respiration assay medium-2 (ERAM-2; Research Institute for the Functional Peptides, Yonezawa, Japan) and dropped individually to the bottom of the microwell. The medium temperature was maintained at 37°C by placing on a warming plate on the microscope stage. The measurement of oxygen consumption was carried out according to the procedure previously described by Shiku et al. (2001). Briefly, Pt-microdisc electrodes, sealed in a tapered soft-glass capillary (PG10165-4; World Precision Instruments, Sarasota, FL), were fabricated according to the procedure described by Matsue et al. (1993). The tip potential was held at −0.6 V versus Ag/AgCl with a potentiostat to monitor the local oxygen concentration in the solution. The tip scanning rate was 31.0 μm/sec. The XYZ-stage and the potentiostat were controlled by a notebook computer. Voltammetry of the Pt-microdisc electrode in ERAM-2 solution showed a steady-state oxygen reduction wave. No response from other electrochemically active species was observed near the embryo surface. The oxygen consumption rate of embryos was calculated by software, in which the oxygen concentration difference between the bulk solution and sample surface (ΔC), and the oxygen consumption rate (F) of a single sample were estimated according to spherical diffusion theories (Shiku et al., 2001). We repeatedly scanned the electrode back and forth, three times, to estimate the mean ± standard deviation ($n \geq 4$) of the ΔC for each sample.

Differential staining

The cell allocation of blastocysts was assessed by differential staining of the inner cell mass (ICM) and trophectoderm (TE) cells according to the staining procedure described by Thouas et al. (2001) with slight modification. Briefly, TE cells of the blastocysts were stained with 100 μg/mL propidium iodide fluorochrome containing a permeabilizing solution of 2% (v/v) Triton X-100 ionic detergent for 20 sec. Blastocysts were then incubated overnight at 4°C in a second solution of 25 μg/mL Hoechst 33342 in ethanol for fixation. Fixed and stained whole blastocysts

were mounted and assessed for cell number using an epifluorescence microscope.

Detection of apoptosis-positive cells by TUNEL assay

Detection of apoptosis-positive cells by TUNEL assay was performed as described by Yamanaka et al. (2009). Blastocysts from SCNT and IVF were washed three times in PBS supplemented with 0.1% polyvinylpyrrolidone and fixed in 2% (w/v) paraformaldehyde and 0.2% (v/v) Triton-X PBS solution for 40 h at room temperature (RT). A commercially available kit (ApopTag; Intergen, Purchase, NY, USA) was used for the detection of apoptosis-positive cells. For the positive control, blastocysts were treated with DNase I (10 IU/mL, Sigma). After washing with PBS supplemented with 0.1% (w/v) polyvinyl alcohol three times for 10 min each, the blastocysts were incubated in the equilibration buffer of the kit for 20 sec at RT. Then, they were incubated at 37°C for 2 h in a moist chamber with 70% (v/v) reaction buffer containing 30% (v/v) terminal deoxynucleotidyl transferase, digoxigenin-11-dUTP. The reaction was stopped by addition of 3% (v/v) stop/wash Buffer (Intergen) at 37°C for 10 min. After washing with PBS including 0.2% Triton-X for four times for 2 min each, they were incubated with antidigoxigenin antibody conjugated to horseradish peroxidase at RT for 1 h. After washing with 0.2 % Triton-X and 0.1% PVA PBS four times, blastocysts were stained with 10 μg/mL propidium iodide in PBS for 1 h at RT. All samples were examined under a laser-scanning confocal microscope (MCR-1024; BIO-RAD Hercule). The numbers of apoptosis-positive nuclei and total number of nuclei in blastocysts were determined.

Individual culture of blastocysts

At day 5 after *in vitro* culture, the blastocysts were collected and washed three times in 100-μL droplets of PZM-3. Thereafter, they were individually cultured in 96-well plates containing 100 μL of PZM-3 for 48 h at 38.5°C in 5% CO_2 in humidified air. The individual culture system was used in Experiments 4 and 5 (shown in Figs. 2, 3, and 4). Both IVF and SCNT blastocysts derived from the individual culture system did not differed from those of conversional group culture system, which was used in Experiment 7 (shown in Table 5), on the embryo cell numbers and apoptosis incidence.

Experimental Studies

In Experiment 1, the rates of cleavage and blastocyst formation in IVF and SCNT embryos were assessed on day 2 and on days 5, 6, and 7 (the day of IVF was defined as day 0) of *in vitro* culture, respectively. In each trial, IVF and SCNT embryos were cultured in each drop.

In Experiment 2, oxygen consumption in the preimplantation IVF and SCNT embryos was measured at the two-cell stage on day 1 (2C); four-cell stage on day 2 (4C); morula stage on day 4 (MO); and blastocyst stages on days 5 (D5BL), 6 (D6BL), and 7 (D7BL). In each trial, IVF and SCNT embryos were cultured in each drop, and measured oxygen consumption at each stage. Some of embryos measured oxygen consumption at D5BL, D6BL, and D7BL were counted total cells number with Hoechst 33342 for calculating oxygen consumption per one cell. As physiological control, *in vivo* produced embryos at molura stage on day 4 (MO) and blastocyst stage on day 5 (D5BL) were also measured oxygen consumption.

In Experiment 3, to further explore some of the possible causes of lower oxygen consumption in the SCNT embryos, we examined the effects of the following four parameters on oxygen consumption of SCNT embryos: removal of ooplasm, contamination of cytoplasm of the donor cell, method of nuclear transfer (microinjection or electrofusion), and artificial activation. In each trial, IVF, PA, Sham-PA, SCI-PA, IN-SCNT, and EF-SCNT embryos were cultured in each drop. The embryos at D5BL were measured for oxygen consumption and then counted for total cell numbers with Hoechst 33342.

In Experiment 4, we determined the correlation between oxygen consumption in embryos at D5BL and their subsequent hatching competence at D7BL. In each trial, IVF and SCNT embryos were cultured in each drop and oxygen consumption was measured at D5BL. Furthermore, these blastocysts were individually cultured, and the developmental stage—unexpanded, expanded (i.e., expansion of the blastocoele and decrease in the thickness of the zona pellucida), hatching (i.e., hatching of the embryos from the zona pellucida), and hatched (i.e., those embryos that had hatched from the zona pellucida) (Kameyama, 1998)—was assessed at 48 h after extended culture (D7BL). Expanded and hatching of SCNT could not be strictly assessed. This was because the SCNT embryos already had mechanical slits or holes in their zona pellucid.

In Experiment 5, to gain an in-depth understanding of the reason behind the lower oxygen consumption in the SCNT embryos, we focused on the total, ICM, and TE cell numbers and apoptosis incidence of embryos. First, we examined the total, ICM, and TE cell numbers and apoptosis incidence of embryos at D5BL and D7BL. In each trial, IVF and SCNT embryos were cultured in each drop and oxygen consumption was measured at D5BL. Next, we determined the correlation between oxygen consumption in embryos at D5BL and their total, ICM, and TE cell numbers and at D7BL. In each trial, IVF and SCNT embryos were cultured in each drop and oxygen consumption measured at D5BL. Furthermore, these blastocysts were individually cultured, and total, ICM, and TE cell numbers and apoptosis incidence were assessed at D7BL.

In Experiment 6, to evaluate whether oxygen consumption was altered by the difference in donor cell types such as pFF and pCC, the effect of donor cells on oxygen consumption in SCNT embryos at D5BL was studied. In each trial, IVF and three types of SCNT (pFF, pCC-Auto, and pCC-Allo) embryos were cultured in each drop. The embryos at D5BL were measured oxygen consumption and then counted total cells number with Hoechst 33342.

In Experiment 7, hatchability, embryo cell numbers and apoptosis incidence of SCNT embryos with pFF and pCC at D7BL was evaluated. In each trial, two types of SCNT (pFF and pCC) embryos were cultured in each drop. SCNT embryos with pCC were derived from both pCC-Auto and pCC-Allo. On the days specified in Experiment 1, the rates of cleavage and blastocyst formation were calculated. The embryos at D7BL assessed the rate of hatched blastocyst, ICM, and TE cell numbers and apoptosis incidence.

Statistical analysis

Each experiment was performed in at least triplicate. The correlation coefficients between oxygen consumption and cell allocation or apoptosis were determined by simple regression analysis. Percentage data were arc-sine transformed, and other data were analyzed using analysis of variance (ANOVA), followed by the Bonferroni procedure ($p < 0.05$). The statistical significance of all data was examined using StatView (Abacus Concepts Inc., Berkeley, CA, USA).

Results

Experiment 1. In vitro development of porcine IVF and SCNT embryos

The cleavage rate did not significantly differ between the IVF and SCNT embryos (Table 1). On the other hand, at D5BL, D6BL, and D7BL, the blastocyst formation rates in the case of SCNT embryos were significantly lower than those in the case of IVF embryos ($p < 0.05$).

Experiment 2. Oxygen consumption in preimplantation IVF and SCNT embryos

As shown in Figure 1A, oxygen consumption, expressed as mean ± SD, in the preimplantation IVF embryos at the 2C and 4C stages was stable at a low value (0.35 ± 0.12 and $0.38 \pm 0.08 \times 10^{14}$/mol sec^{-1}, respectively). Thereafter, oxygen consumption significantly increased at the MO stage ($0.52 \pm 0.11 \times 10^{14}$/mol sec^{-1}) compared to that at the 2C stage ($p < 0.05$). Subsequently, this value increased 1.5 times at D5BL ($0.82 \pm 0.18 \times 10^{14}$/mol sec^{-1}). In contrast, the SCNT embryos at D5BL did not exhibit any increase in oxygen consumption from the MO stage, even up to D7BL (MO, $0.41 \pm 0.08 \times 10^{14}$/mol sec^{-1}; D5BL, $0.44 \pm 0.12 \times 10^{14}$/mol sec^{-1}; and D7BL, $0.46 \pm 0.11 \times 10^{14}$/mol sec^{-1}) (Fig. 1B). Furthermore, we compared the oxygen consumption calculated by per one cell of the IVF and SCNT embryos at the blastocyst stage (Fig. 1CD). The values in the case of the SCNT embryos were lower than those in the case of the IVF embryos at D5BL, D6BL, and D7BL ($p < 0.05$).

From the MO stage to the D5BL stage, we found the significant difference in the way of changing of oxygen consumption between the IVF and the SCNT embryos (Fig. 1AB). For this confirmation, we further examined the oxygen consumption in *in vivo*-produced embryos at both the MO and D5BL stages. The result revealed that the oxygen consumption in *in vivo* produced embryos increased 1.5 times from the MO stage to the D5BL stage as well as in the IVF embryos (MO: $n = 4$; $0.67 \pm 0.06 \times 10^{14}$/mol sec^{-1} and D5BL: $n = 8$; $0.93 \pm 0.14 \times 10^{14}$/mol sec^{-1}).

Experiment 3. Effect of removal of the ooplasm, contamination of the cytoplasm of the donor cell, method of nuclear transfer, and artificial activation on oxygen consumption at D5BL

As shown in Table 2, there were no significant differences with respect to the oxygen consumption and total cell number of embryos at D5BL between the IVF, PA, Sham-PA, and SCI-PA embryos; further, the values of oxygen consumption were significantly higher in these embryos than in the SCNT embryos ($p < 0.05$). Furthermore, there were no significant differences with respect to the oxygen consumption and total cell number of embryos at D5BL between the method of nuclear transfer; namely, the microinjection (IN-SCNT) and electrofusion (EF-SCNT) methods. Thus, the removal of ooplasm, contamination of the cytoplasm of the donor cell, method of nuclear transfer, and artificial activation did not influence anomalous oxygen consumption in the SCNT embryos.

Experiment 4. Correlation between oxygen consumption at D5BL and subsequent developmental competence

To clarify the correlation between oxygen consumption and subsequent development, the sample embryos that were used for analysis were aligned as previously described (Kameyama, 1998). We selected IVF and SCNT embryos at D5BL with similar morphology—in these embryos, the volume of the blastocoele cavity up to the vacuole was half that of the entire embryo (Fig. 2A). The oxygen consumption (mean ± SD) in the IVF embryos at D5BL definitely reflected their hatching ability at D7BL (Fig. 2B). However, the oxygen consumption was significantly lower at D5BL in the SCNT embryos than in the IVF embryos that underwent expansion at D7BL ($p < 0.05$).

Next, on the basis of the results shown in Figure 2B, oxygen consumption in the IVF and SCNT embryos at D5BL was classified into four classes, as shown in Figure 2C: <0.59, 0.59–0.74, 0.75–0.93, and >0.93×10^{14}/mol sec^{-1}, representing embryos with the potential of undergoing one of the following developmental stages, respectively: unexpanded, expanded, hatching, and hatched. These four groups comprised 15.6, 31.3, 28.1, and 25% of the IVF embryos at D5BL, respectively. In contrast, at D5BL, most of the SCNT embryos were categorized as being in the unexpanded or expanded

TABLE 1. *IN VITRO* DEVELOPMENTAL COMPETENCE OF IVF AND SCNT EMBRYOS

Embryos	No. of embryos cultured	No. (percent ± SD) of embryos cleaved on day 2	No. (percent ± SD) of embryos developed to the blastocyst stage (BL) on		
			Day 5 (D5BL)	Day 6 (D6BL)	Day 7 (D7BL)
IVF	114	84 (74.0 ± 11.1)	37 (33.0 ± 11.8)[a]	47 (41.9 ± 11.8)[a]	47 (41.9 ± 11.8)[a]
SCNT	116	76 (65.4 ± 3.9)	19 (15.9 ± 4.9)[b]	28 (24.0 ± 6.2)[b]	30 (26.0 ± 6.2)[b]

[a–b]Different letters within the same stage indicate significant difference ($p < 0.05$).
IVF, *in vitro*-fertilized; SCNT, somatic cell nuclear transfer.